

Doped magnetic moments in a disordered electron system: insulator-metal transition, spin glass and ‘cmr’

Sanjeev Kumar and Pinaki Majumdar
Harish-Chandra Research Institute,
Chhatnag Road, Jhusi, Allahabad 211 019, India
(January 15, 2001)

Recent experiments on the amorphous magnetic semiconductor Gd_xSi_{1-x} , Phys. Rev. Lett. **77**, 4652 (1996), *ibid* **83**, 2266 (1999), *ibid* **84**, 5411 (2000), *ibid* **85**, 848 (2000), have revealed an insulator-metal transition (i-m-t), as a function of doping and magnetic field, a spin glass state at low temperature, and colossal magnetoresistance close to the i-m-t. There are also signatures of strong electron-electron interaction close to the i-m-t. Motivated by these results we examine the role of doped magnetic moments in a strongly disordered electron system. In this paper we study a model of electrons coupled to structural disorder and (classical) magnetic moments, through an essentially exact combination of spin Monte Carlo and fermion exact diagonalisation. Our preliminary results, ignoring electron-electron interactions, highlights the interplay of structural and magnetic ‘disorder’ which is primarily responsible for the observed features in magnetism and transport.

I. INTRODUCTION

A. Insulator-metal transition in doped semiconductors

The role of disorder in electronic systems is an enduring theme in condensed matter physics¹⁻⁴. Structural disorder leads to localisation of electronic states and, in a three dimensional system, all electronic states would be localised³ if the disorder, ‘ Δ ’ say, were greater than a critical value (Δ_c). For weaker disorder, $\Delta < \Delta_c$, only states *beyond* an energy $\epsilon_c(\Delta)$ of the band center, *i.e* in the band tails, are localised. A system is metallic or insulating depending on whether the Fermi level, ϵ_F , is above or below this ‘mobility edge’ ϵ_c . Variation in electron density, and hence ϵ_F , can drive a system through the i-m-t. This is the basic scenario for the ‘Anderson transition’ in a non interacting electron system^{3,4}.

Doped semiconductors⁵ have served as a laboratory for studying disorder effects since they allow systematic control of the carrier density. The i-m-t has been studied in doped crystalline systems, the most famous example being phosphorus doped silicon⁶ (Si:P), and less extensively in amorphous semiconductors⁷. In experimental systems, however, the phenomena of localisation is complicated by electron-electron (e-e) interaction effects which become very pronounced close to the i-m-t⁸. There are clear signatures of interaction effects in the density of states and the conductivity in amorphous systems close to the i-m-t. The interplay of disorder and interaction effects near the i-m-t is not completely understood^{9,10} and continues to be an area of active research.

The introduction of magnetic moments in a ‘disordered’ system brings in new phenomena. The effects are well understood in crystalline semiconductors^{11,12}, where the disorder is weak and the relevant regime is of low carrier density. In these systems, electrons are trapped in

the potential fluctuations and polarise the magnetic moments in their neighbourhood. This leads to a gain in exchange energy, and tends to enhance the localisation of the carrier. The net localising effect in these systems, therefore, arises from a combination of (i) on site disorder; a ‘single particle’ effect, and (ii) ‘bound state’ formation between the electron and the magnetic moments; a ‘many body’ effect. The composite object, a (trapped) electron and the polarised spins in its vicinity, is called a ‘spin polaron’. Since the i-m-t in these systems occurs at a carrier density $\sim 10^{-5}$ (per unit cell), the picture of non overlapping, uncorrelated, spin polarons is adequate. The interesting difference between these systems and their non magnetic counterparts lies in the response to a magnetic field. An applied field globally aligns the magnetic moments, reduces the polaron binding energy, and tunes the ‘magnetic component’ of localisation. The change in activation energy (or mobility) of the carriers can lead to *enormous magnetoresistance*^{13,14}. These systems have been known to exhibit ‘colossal magnetoresistance’ (cmr) much before such effects were observed in the manganites.

Recent experiments¹⁵⁻¹⁸ on amorphous (*a*)-GdSi reveal that doping magnetic moments in an *amorphous* system combines the richness, and complication, of the traditional i-m-t in amorphous semiconductors⁷ with the physics of ‘cmr’. In addition a disordered magnetic state, a spin glass, with rather unusual properties emerges at low temperature. This combination of an i-m-t, in a high carrier density system, with cmr, and a spin glass ground state is probably unique to GdSi. We will discuss these experiments in the next section. The essential phenomena in these systems seems to be: (i) electron localisation due to the strong disorder in the amorphous structure, (ii) indirect exchange interaction between the doped moments, mediated by the electrons, leading to a spin glass state, (iii) feedback of the spin background

on the electronic system, via ‘spin disorder’, tending to enhance electron localisation, (*iv*) strong e-e interactions in the vicinity of the i-m-t, showing up as a correlation gap in the density of states, a \sqrt{T} dependence of the low temperature conductivity, and ‘local moment formation’ in the electron system, and, (*v*) control of the ‘spin disorder’ by a magnetic field, h , leading to large negative magnetoresistance when the electron density is close to the critical density.

Unlike the case of crystalline magnetic semiconductors, where the picture of isolated ‘bound magnetic polarons’^{11,12} seems to suffice, we do not have an understanding of a *high density of electrons in the background of strong disorder, interacting with randomly located magnetic moments and with each other*. Scenarios in terms of an Anderson transition, or isolated polarons, or model spin glasses, do not suffice, and the interplay of these effects is what we study in this paper.

While we are motivated by the phenomena in GdSi, which we take to be the prototype amorphous magnetic semiconductor, our focus in this paper differs from the experiments in two respects. (*i*) In the experiments, discussed later, the tunable parameters are the electron density (n_{el}) and the density of doped magnetic moments (n_{sp}). Carrier density and ‘moment density’, however, are not independent variables since both come from the doped Gd atoms. Thus, $n_{sp} \sim n_{el}$ and most of the data is for $n_{sp} = x \sim x_c$, with variations of a few percent. The ‘disorder’ (Δ) due to the amorphous structure, or the coupling (J) between the electron and doped moments cannot be varied experimentally. We will discuss a model which is expected to describe GdSi (see later) but not restrict ourself to parameters specific to the real system right away. The model has a large parameter space and we will explore it gradually to locate some of the phenomena, i-m-t, spin glass and ‘cmr’, mentioned earlier. We will present our results specific to GdSi in a separate publication¹⁹. (*ii*) The effects in GdSi arise from a combination of structural disorder, electron-spin interaction, and e-e interaction. All of them are important, in varying degrees, for the phenomena observed. We will study a *model problem* of electrons coupled to structural disorder and magnetic moments, and ignore e-e interactions in the present discussion. They are important, as we will see in a detailed review of the experiments, but we have a non trivial problem even without such interactions. As far as we know even this simplified model has not been explored. We will estimate and quantify the e-e interaction effects in our results specific to GdSi¹⁹.

Here is the outline of the text. In the next section we discuss the experimental results on amorphous (*a*)-GdSi in some detail, to highlight the effects of doping magnetic moments into a disordered system. Following that we define a model which we believe contains most of the relevant physics. We then discuss the approximations involved in ‘solving’ for the properties of this model and present results on the magnetic properties, thermodynamics, and some simple limits for the conductivity.

We conclude by indicating how electron-electron interaction effects can be included, approximately, within our scheme. This would recover some of the features in the experimental data which are not accessible in our ‘non-interacting’ model.

B. Magnetic moments in an amorphous background: experiments

Treating GdSi as the ‘model’ amorphous magnetic semiconductor we review some of the effects which have been experimentally observed. The measurements have been made^{15–18} on *a*-GdSi and simultaneously on the *non-magnetic analog a*-YSi, to clarify the role of magnetic moments on the i-m-t. The results are broadly on (*i*) the conductivity, σ , and the magnetoresistance, (*ii*) spectral properties/density of states (DOS), probed through tunneling, (*iii*) thermodynamic properties: specific heat, C_V , and entropy, S , and (*iv*) magnetic properties: the linear response susceptibility $\chi(T)$ and the magnetisation $m(h, T)$.

Let us begin by with the conductivity¹⁵. (*a*). Both Y_xSi_{1-x} and Gd_xSi_{1-x} show an insulator-metal transition as the doping, x , is increased across a critical value x_c . The critical doping required ($x_c \sim 14\%$) is slightly greater in GdSi compared to YSi. (*b*). For both GdSi and YSi, in the doping range $0.17 > x > 0.11$, the conductivity has $d\sigma/dT > 0$, *i.e.* $d\rho/dT < 0$, at all T . This is true even of the systems which are ‘metallic’ at low temperature. (*c*). For the metallic samples the low temperature conductivity can be fitted to $\sigma(T) \sim \sigma_0 + \sigma_1\sqrt{T}$. σ_0 and σ_1 are constants and the \sqrt{T} term arises from Coulomb effects in a disordered system⁸. On the insulating side $\sigma(T) \sim e^{-\sqrt{T_0/T}}$, indicating variable range hopping (VRH) in the presence of a soft Coulomb gap²⁰. (*d*). All Gd based systems, in the doping range studied, show pronounced negative magnetoresistance (MR). The MR increases on reducing x (towards x_c), on decreasing T , and on increasing h . YSi samples of comparable composition show a significantly smaller, *positive*, MR. (*e*). The field dependence of conductivity is seen to arise principally from variations in σ_0 in the metallic phase²¹, and from the variation of T_0 in the insulator²². So, the dominant *temperature dependence* of the conductivity in the metallic phase arises from Coulomb effects, driving the \sqrt{T} , *but the MR arises almost entirely from variations in the $T = 0$ conductivity*. (*f*). For GdSi samples with $x \lesssim x_c$ an applied magnetic field can drive the system metallic. Near this field driven i-m-t, σ_0 varies as $(h - h_c)$, h_c being the field at which the i-m-t occurs. The effects, (*a*) and (*d*) – (*f*), hint at the crucial role of magnetic moments in determining electronic transport.

The low energy DOS has been studied¹⁸, from measurement of the tunneling conductance, across the field driven i-m-t. These measurements provide direct information on the evolution of the correlation gap⁸ (dip

in DOS at ϵ_F) near the metal-insulator transition and the Coulomb gap²⁰ in the insulating phase. The principal conclusion from these measurements is that, for the field tuned transition, the density of states at the Fermi level, $N(0)$, varies as $(h - h_c)^2$ while $\sigma_0(h) \sim (h - h_c)$. Therefore, the critical behaviour near the i-m-t follows $N(0) \propto \sigma^2$, with both the DOS and the d.c conductivity vanishing at the transition.

The difference in the thermodynamic properties of magnetic and non magnetic systems again emphasises the role of the doped moments. Even for disordered ‘non-magnetic’ systems close to the metal-insulator transition the specific heat has a contribution arising from ‘local moments’²³. This arises because electrons can behave like *localised* $S = 1/2$ *objects* in the presence of disorder and strong e-e interactions²⁴. However, after ‘subtracting out’ the specific heat of the non magnetic analog, one would expect the ‘high temperature’ entropy of the magnetic system to correspond to $S^0(\infty) \sim n_{sp} \log(2S + 1)$. Results on GdSi differ from this: (a). Specific heat measurements indicate that at ‘high’ temperature $S_{mag}(T) = \int_0^T dT' C_V^{mag}/T'$ is larger¹⁶ than $S^0(\infty)$ by approximately 50%! The total magnetic entropy tends to saturate, at this (larger) value by $T \sim 60 - 70$ K. A simple minded estimate¹⁶ suggests that the additional entropy can be accounted for by ~ 2 spin $1/2$ moments (conduction electrons) for each Gd moment. (b). C_V^{mag} should vanish as $T \rightarrow 0$, however, down to 5 K, it shows *no sign of a downturn*¹⁶. This suggests that the peak in C_V^{mag} occurs somewhere below 5 K. At high temperature the magnetic and non magnetic systems have the same C_V .

Finally, the magnetism. The doped Gd atoms possess a moment $J = S = 7/2$, arising from the half-filled f shell. The coupling between the randomly located moments arises primarily through mediation by the conduction electrons. The overall magnetic effects also have contributions from the ‘local moments’ in the conduction electron system, alluded to in the previous paragraph. The basic observations on the magnetism are: (a). Measurements at high fields, $h \sim 1$ T, show a magnetisation growing as $\sim 1/T$, *i.e.* free moment like response. However, measurements of χ at low field ($h \sim 10$ mT), reveals a transition¹⁷ to a spin glass state at a temperature $T_f \sim 1-6$ K depending on doping. (b). The freezing temperature increases from $T_f \sim 1$ K at $x = 0.04$ to $T_f \sim 6$ K at $x \sim 0.20$. The observation of the characteristic²⁵⁻²⁷ (logarithmic) frequency dependent shift of T_f confirms that these are indeed spin glasses. (c). There is a distinct difference between the field cooled (FC) and zero field cooled (ZFC) susceptibilities $\chi(T)$; the FC susceptibility saturates to a higher value as $T \rightarrow 0$. (d). Fitting a Curie form to the susceptibility, $\chi(x, T) = A(x)/(T - \theta(x))$, reveals that the effective moment, μ_{eff} , which can be extracted from A , varies significantly with x . Naively, this should have been just $\sqrt{S(S + 1)}$, independent of x . It is close to this expected (free moment) value for $x \approx x_c$ and falls off on both the metallic and insulating sides.

(e). The spin glass freezing does not have any signature in the temperature dependence of transport properties. The freezing itself is eliminated by fields $h \gtrsim 0.1$ T.

These results suggest that the magnetic state, which crucially affects electronic transport, is itself determined by electron spin interaction, the background disorder, and e-e effects.

Let us abstract our lessons from these effects, to start on a theory. The *primary* effect in amorphous magnetic systems is electron localisation due to disorder, either due to randomness in the amorphous structure or disorder in the spin configuration. To a first approximation, the i-m-t is driven by varying the mobility edge ϵ_c across ϵ_F . However, as the data indicates, the transition is not a simple ‘Anderson transition’, driven by structural and spin disorder, in a non-interacting electron system. Electron-electron interaction effects are clearly in evidence in (i) the temperature dependence of $\sigma(T)$, (ii) low energy features in the DOS, $N(\epsilon)$, and, possibly also in (iii) the ‘excess entropy’, at high temperature, and (iv) the non monotonic variation in μ_{eff} across the i-m-t.

The transition, however, is not driven by interaction effects *per se*. Interactions become relevant near the transition, there the effects of disorder and interactions cannot be deconvolved, but most of the phenomena occur *because the system is strongly disordered*. Since we will study a model without e-e effects, note that many of the experimental results *can be understood*, at least qualitatively, even without such interaction. These include (i) the *existence* of an i-m-t, from variation in the ‘effective disorder’ seen by the electron, (ii) a magnetically disordered ground state and the spin glass signatures, and, (iii) the large MR from the field tuning of spin disorder.

This problem, even without Coulomb effects, is non trivial because: (a) there is no simple method for accessing transport properties in the regime we are interested in (even if the ‘disorder’ were completely specified), and (b) the ‘spin disorder’ is *not specified*, the magnetic state itself depends intimately on the electronic spectrum and wavefunctions. This coupling is at the heart of the problem.

II. THE MODEL

The model for amorphous magnetic semiconductors would have the form

$$H = \sum_{ij} (t_{ij,\sigma} c_{i\sigma}^\dagger c_{j\sigma} + h.c.) - \sum_i \mu n_i + J' \sum_\nu \sigma_\nu \cdot \mathbf{S}_\nu + \sum_{ij} V_{ij} n_i n_j \quad (1)$$

where the label i, j etc refer to the (non periodic) atomic locations $\mathbf{R}_i, \mathbf{R}_j$ etc. The labels ν refer to some set of positions $\{\mathbf{r}_\nu\}$, say, where the magnetic ions are located. The t_{ij} would have a distribution since the structure is

non crystalline. The V_{ij} stand for the Coulomb interaction. σ_ν is the electron spin operator and we have assumed the local electron-spin coupling, J' , to be site independent.

A simpler variant of this model, presumably with similar physics, is the following:

$$H = -t \sum_{\langle ij \rangle, \sigma} (c_{i\sigma}^\dagger c_{j\sigma} + h.c.) + \sum_{i\sigma} (\epsilon_i - \mu) n_{i\sigma} + J' \sum_{\nu} \sigma_\nu \cdot \mathbf{S}_\nu + \sum_{ij} V_{ij} n_i n_j \quad (2)$$

Here the i, j refer to sites on a *periodic structure* and the t now refers to nearest neighbour hopping on that lattice. The ‘amorphous’ nature is incorporated via the random on site potential, ϵ_i , and the sites $\{\mathbf{r}_\nu\}$ are some subset of the lattice points $\{\mathbf{R}_i\}$. The parameters of the theory are t , $\langle \epsilon_i^2 \rangle = \Delta^2$, J' , $n_{el} = N_{el}/N$ and $n_{sp} = N_{spin}/N$. N is the size of the system. After normalising by t there are two ‘coupling constants’, Δ/t and J'/t , and two ‘densities’: four dimensionless system parameters in all. We will measure all energies in units of t which, from hereon, is set to 1. The Coulomb term, even if included, does not involve a variable coupling constant. In addition to all these there are temperature and magnetic field as external variables. In what follows we will ignore the Coulomb term. We will also treat the core spin \mathbf{S}_i as ‘classical’, and study the magnetic properties, thermodynamics, and some aspects of transport in this model.

III. COMPUTATIONAL SCHEME

Having defined the Hamiltonian we have to adopt a scheme for evaluating its properties. The problem involves strong disorder, in the variables $\{\epsilon_i\}$, as well as temperature (and field) dependent ‘disorder’ in the spin background $\{\mathbf{S}_i\}$. Part of the problem is to determine the distribution of spin configurations, appropriate to a given T and h , the rest to calculate and average electronic properties over the disorder (on site & spin). In the regime we are interested in, *neither of these tasks is analytically tractable*. Thankfully, there is an essentially exact, and implementable, numerical scheme which can be employed here. This is what we discuss next.

Consider the model for some arbitrary coupling J' and disorder Δ . The spins are considered to be classical (formally, $S \rightarrow \infty$). The problem looks like quadratic (non interacting) fermions in the background of a spin configuration $\{\mathbf{S}_i\}$. The task is to determine the appropriate background configuration(s), $\{\mathbf{S}_i\}$, at a given temperature and specified values of the electronic parameters. The problem can be set up formally as follows: Consider a Hamiltonian $H = H_{el} + J' \sum_i \sigma_i \cdot \mathbf{S}_i$. Here H_{el} is a quadratic fermion Hamiltonian excluding terms involving the \mathbf{S}_i 's. The partition function of this system is:

$$Z = \int \mathcal{D}\mathbf{S}_i \text{Tr}_{c,c^\dagger} e^{-\beta(H_{el} + J' \sum_i \sigma_i \cdot \mathbf{S}_i)} \quad (3)$$

We can formally trace over the fermions and write the partition function purely as an integral over spin configurations, *i.e.*,

$$Z = \int \mathcal{D}\mathbf{S}_i e^{-\beta H_{eff}\{\mathbf{S}_i\}} \quad (4)$$

where the effective ‘spin Hamiltonian’, H_{eff} , satisfies

$$e^{-\beta H_{eff}} = \text{Tr}_{c,c^\dagger} e^{-\beta(H_{el} + J' \sum_i \sigma_i \cdot \mathbf{S}_i)} \quad (5)$$

It is obvious that the functional $H_{eff}(\{\mathbf{S}_i\})$ is just the fermion free energy F_{el} in the background $\{\mathbf{S}_i\}$. In general it depends on the full *spin configuration* $\{\mathbf{S}_i\}$ and not just pairwise interactions. Our problem ‘reduces’ to fermions in the background of some quenched disorder, exchange coupled to spins *picked from a distribution* $P(\{\mathbf{S}_i\}) \propto e^{-\beta H_{eff}(\{\mathbf{S}_i\})}$. To calculate physical properties involving the fermions, the DOS or conductivity, say, we have to average over spin configurations picked from the distribution P appropriate to a given temperature. The temperature dependence and the spin-spin correlations implicit in P indicate that the ‘disorder’ arising from the J' term is very different from the quenched uncorrelated disorder in the ϵ_i 's.

Loosely, the fermion properties can be calculated by (weighted) average over probable spin configurations. The weights themselves depend on a knowledge of the fermion free energy in a given configuration! We have a coupled problem here, and need to solve it self consistently.

A. Exact enumeration

We have written a formal prescription for the spin distribution: how do we proceed any further? A computational scheme has been developed and explored over the last few years for handling this kind of problems^{28,29}. Starting with some arbitrary configuration $\{\mathbf{S}_i\}_0$, the Metropolis algorithm is used for updating the spin orientations and generating new (acceptable) configurations. The acceptance or rejection of a spin move, which depends on nearest neighbour orientations in short range spin models, *now involves the diagonalisation of a $N \times N$ fermion Hamiltonian*. Unless some approximations can be made, simulating such a model involves computational effort of $\mathcal{O}(N^4)$, where N is the system size. A factor of N^3 comes from each diagonalisation (acceptance/rejection of a spin ‘move’) and another N from the need to ‘update’ all N spins in the system. This N^4 process has to be repeated $\sim 10^3 - 10^4$ times at each temperature for equilibration and averaging over equilibrium configurations. At equilibrium, the spin configurations generated are a sampling of $P(\{\mathbf{S}_i\})$. Fermion averages calculated over these configurations represent equilibrium average at that temperature. While this scheme

is ‘exact’, and has no sign problems unlike fermion QMC, the cost for handling large systems is still prohibitive. On a standard DEC Alpha workstation one can handle systems $\sim 4 \times 4 \times 4$ i.e $N \sim 100$. Working out the temperature dependence of χ , say, for fixed electronic parameters, involves about 12 hours of CPU time. The largest system studied³⁰ is 6^3 for the double exchange model. To get a first impression of these complicated systems, the thermodynamics and energetics of various phases can be reasonably studied for these small sizes. However, where transport studies are of interest, and they are the most interesting measurable property in these systems, the accessible sizes are much too small for making useful statements (about σ_{dc} , say). This is because the mean free path l_{mfp} in the low resistivity phases is often larger than the system size ($l_{mfp} \gtrsim L$) and no useful statements can be made about the conductivity of the thermodynamic system. Some advances have been made by (i) making the algorithms more efficient than N^4 , and (ii) using ‘effective’ spin models for generating $P(\{\mathbf{S}_i\})$, rather than handling the full $H_{eff}(\{\mathbf{S}_i\})$. Algorithms in the first category are rather complex and still in an experimental phase^{31,32}, while for approximations in the second category there is often no obvious small parameter. In this study we use an approximate scheme, described in the next section, after benchmarking it against small system simulations based on the exact scheme.

B. Perturbative expansion in J'

While there is no obvious approximation for arbitrary values of the quenched disorder Δ and the exchange coupling J' , the experimentally relevant regime in J' (see later) allows a controlled approximation. We have argued that $P(\{\mathbf{S}_i\}) \propto e^{-\beta E_{el}(\{\mathbf{S}_i\})}$. Let us, for simplicity, look at $T = 0$, in which case $P(\{\mathbf{S}_i\}) \propto e^{-\beta E_{el}(\{\mathbf{S}_i\})}$. If the coupling J' were small, in a sense to be quantified soon, we can try expanding the energy $E_{el}(\{\mathbf{S}_i\})$, about the $J' = 0$ limit, in powers of J' . This is just quantum mechanical second order perturbation theory, estimating the change in ground state energy of the electrons due to coupling to an *arbitrary* spin configuration. It is a variant of the textbook ‘RKKY’ argument^{33,34} and we briefly describe the steps below.

The reference system (at $J' = 0$) is spin degenerate, so $\langle \sigma_i^\mu \rangle_0 = 0$, for $\mu = x, y, z$, and there is no $\mathcal{O}(J')$ contribution to the energy. The $\mathcal{O}(J'^2)$ term is

$$\Delta E_0(\{\mathbf{S}_i\}) = \sum_{m \neq 0} \frac{|\langle \Psi_0^N | J' \sum_i \sigma_i \cdot \mathbf{S}_i | \Psi_m^N \rangle|^2}{E_0^N - E_m^N} \quad (6)$$

The $|\psi\rangle$'s are many particle wavefunctions (Slater determinants) including the effect of on site disorder. The label N refers to particle number here (not system size) and m is the label for the state. E_0 and E_m refer to (unperturbed) ground state and excited state energies of the N electron system. Writing out the energy change;

$$\begin{aligned} \Delta E_0(\{\mathbf{S}_i\}) &= \sum_{m \neq 0} \frac{\langle \Psi_0^N | J' \sum_i \sigma_i \cdot \mathbf{S}_i | \Psi_m^N \rangle \langle \Psi_m^N | J' \sum_j \sigma_j \cdot \mathbf{S}_j | \Psi_0^N \rangle}{E_0^N - E_m^N} \\ &= J'^2 \sum_{i,j} \sum_{m \neq 0} \frac{\langle \Psi_0^N | \sigma_i \cdot \mathbf{S}_i | \Psi_m^N \rangle \langle \Psi_m^N | \sigma_j \cdot \mathbf{S}_j | \Psi_0^N \rangle}{E_0^N - E_m^N} \\ &= \sum_{ij} J_{ij} \mathbf{S}_i \cdot \mathbf{S}_j \end{aligned} \quad (7)$$

where

$$J_{ij} = J'^2 \sum_{m \neq 0} \frac{\langle \Psi_0^N | \sigma_i^\mu | \Psi_m^N \rangle \langle \Psi_m^N | \sigma_j^\mu | \Psi_0^N \rangle}{E_0^N - E_m^N} \quad (8)$$

The μ label in σ could be x or y or z (not summed over). A large part of ΔE actually comes from the local, S_i^2 , term but that is a constant and does not affect the ‘cost’ of rotating a spin with respect to its neighbours. In defining the effective spin Hamiltonian we look only at the $i \neq j$ terms in ΔE .

To calculate J_{ij} , suppose the single particle wavefunctions of the reference (disordered) electron problem are of the form $\gamma_{\alpha\sigma}^\dagger |0\rangle = A_i^\alpha c_{i\sigma}^\dagger |0\rangle$ and the inverse is $c_{i\sigma}^\dagger = B_i^\alpha \gamma_{\alpha\sigma}^\dagger$. Since A is a ‘rotation matrix’ we will have $B = A^{-1} = A^{T*}$. The intermediate state $|\Psi_m^N\rangle$ is created by a particle-hole creation operator, of the form $\gamma_\alpha^\dagger \gamma_\beta$, acting on $|\Psi_0^N\rangle$ so it is indexed by two labels $\alpha, \beta, \alpha \neq \beta$. Using this notation the exchange constants are specified as

$$J_{ij} = \frac{J'^2}{4} \sum_{\alpha \neq \beta} \{B_i^\alpha B_i^{\beta*} B_j^{\alpha*} B_j^\beta + c.c\} \left(\frac{n_\alpha - n_\beta}{\xi_\alpha - \xi_\beta} \right) \quad (9)$$

The ξ 's are single particle energies and the n are Fermi factors. It can be easily shown that J_{ij} is $J'^2 \chi_{ij}(\omega = 0)$ where χ_{ij} is the spin susceptibility (response function) of the electron system. For electrons in free space this is just the Fourier transform of the standard ‘polarisability’ $\chi_0(\mathbf{q})$. The (inverse) energy scale for χ_0 is $\sim N(\epsilon_F)$, i.e we may write $\chi_0(\mathbf{q}) = N(\epsilon_F) f_0(\mathbf{q})$ where f_0 is a dimensionless function $\mathcal{O}(1)$. Using this, the typical magnitude of the (nearest neighbour) exchange constant is $\sim J'^2 N(\epsilon_F)$.

Using similar arguments on a lattice, the exchange coupling between nearest neighbour spins (on the lattice) will be $\sim J'^2/W$, since $N(\epsilon_F) \sim 1/W$ where W is the bandwidth. In the disordered electron system such a simple identification is no longer possible but the typical nearest neighbour coupling will still be $\sim J'^2 N(\epsilon_F)$.

It is apparent that if J' were small there would be a *hierarchy* of energy scales which may help us in analytically defining the effective spin Hamiltonian. If $J' \ll t$ then for the ‘clean’ electron system we will have $t \gg J' \gg J_{ij}$, while for the disordered problem we will have $\Delta \gtrsim t \gg J' \gg J_{ij}$. Experimentally the value of J' is estimated¹⁷ to be $\lesssim 50$ K. Even with a modest

$t \sim 1000$ K, we would have $N(\epsilon_F)J' \sim 0.05 \ll 1$. We will use a slightly larger J' , *i.e.* $J'/t \sim 0.2$, and the smallness of $N(\epsilon_F)J'$ will allow us to work with a quadratic spin Hamiltonian. Higher order couplings, between three spins etc, will be smaller by this factor.

The primary scheme, as outlined at the beginning of this section, is to average electronic properties by diagonalising the electronic part with spin configurations chosen from the appropriate distribution. In our approximation, the spin distribution is *specified* as $P \propto e^{-\beta H_{sp}}$, where $H_{sp} = \sum_{i \neq j} J_{ij} \mathbf{S}_i \cdot \mathbf{S}_j$, and *does not have to be numerically evaluated*. However, we still have to do a Monte Carlo (MC), with long range spin-spin interactions, to generate the equilibrium spin configurations. The problem involves the following steps now, (i) specify the exchange constants in terms of the spectrum and eigenfunctions of the reference ‘site disorder’ problem, (ii) perform classical Monte Carlo on the spin model to generate a set of equilibrium configurations, in effect a sampling of $P(\{\mathbf{S}_i\})$. (iii) at a given temperature, after the spin system equilibrates, diagonalise the electron problem with some of the spin configurations, and average the computed correlation functions. (iv) since there is quenched disorder in the problem, repeat this entire process for several realisations of $\{\epsilon_i\}$ and average the observables.

If the ‘rotation cost’ etc can be described by a quadratic Hamiltonian then ‘polaronic’ effects, which imply that spin rotation energy depends on the presence or absence of an electron nearby, are *irrelevant*. Polaronic effects may be relevant, *at large* J' , even in high carrier density systems³⁰. The smallness of $N(\epsilon_F)J'$ ensures that such effects are not relevant here.

IV. RESULTS AND DISCUSSION

We now present our results, starting with a comparison of the ‘exact’ and ‘approximate’ schemes for our choice of J' . We then discuss results on the d.c conductivity, in simple situations where the spin distribution does not have to be evaluated through simulation. These data, nevertheless, highlight the interplay of structural and spin disorder, and provide an estimate of the obtainable MR. We finally examine simulation results for magnetic moments in a (progressively) disordered electronic background and the spin glass signatures therein.

A. Comparison of the exact and perturbative schemes

Second order perturbation theory in J' should be sensible as long as $N(\epsilon_F)J' \ll 1$. We have argued that J' is small for the systems of interest. There are two consequences of this. (i) It is an enormous technical simplification because it ‘deconvolves’ the magnetic problem

from the electronic one. For a given electron density, and a realisation of disorder, we only need to compute the exchanges, J_{ij} , once and then work with the resulting H_{sp} . Electronic properties can be calculated by diagonalising the fermion Hamiltonian with configurations $\{\mathbf{S}_i\}$ generated by equilibrating H_{sp} . The computational cost reduces from N^4 , for the exact scheme, to N^2 . In this N^2 , one factor of N is to evaluate the rotation cost for a single spin (in our long range model) another N to update all the spins. (ii) Physically it implies that ‘polaronic’ effects, mentioned earlier are not relevant in this parameter regime. The question of a ‘dense polaron system’ does not arise here.

The single spin rotation cost is the central quantity in the simulation. To emphasise that this energy, at small J' , can be very accurately calculated from H_{sp} we have extensively studied this ‘rotation cost’ under various conditions. Fig.1 illustrates some of the cases. The energy cost of rotation is the difference between the fermion energies $E\{\mathbf{S}_i^1\} - E\{\mathbf{S}_i^0\}$, in the exact scheme, or $H_{sp}\{\mathbf{S}_i^1\} - H_{sp}\{\mathbf{S}_i^0\}$, in the approximate one. $\{\mathbf{S}_i^0\}$ and $\{\mathbf{S}_i^1\}$ are two spin configurations connected by a single spin rotation $\delta\mathbf{S}_j$, say. Fig.1 illustrates three cases. In each of them a reference configuration $\{\mathbf{S}_i^0\}$ is chosen and E and H_{sp} are computed. A rotation is made, changing $\{\mathbf{S}_i^0\}$ to $\{\mathbf{S}_i^1\}$ and E and H_{sp} are computed on this state. We plot $E_1 - E_0$ and $H_{sp}^1 - H_{sp}^0$ as a function of J' for three reference configurations. The reference configuration $\{\mathbf{S}_i^0\}$ is random for the circle and square, it is ferromagnetic for the triangle.

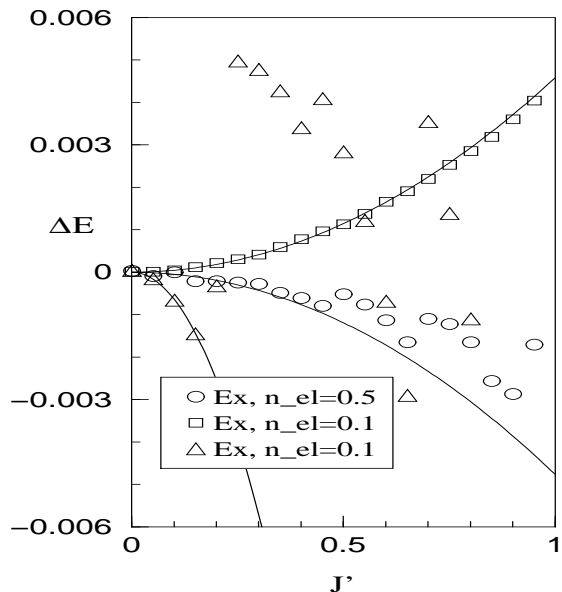


FIG. 1. Energy cost for rotation of a single spin: exact -vs- approximate schemes. The energy difference between two spin configurations is computed through direct diagonalisation (symbols) and by using H_{sp} (lines), as a function of J' . The configurations are described in the text. Disorder: $\Delta = 8$, system size $14 \times 4 \times 4$. There is a spin at each site.

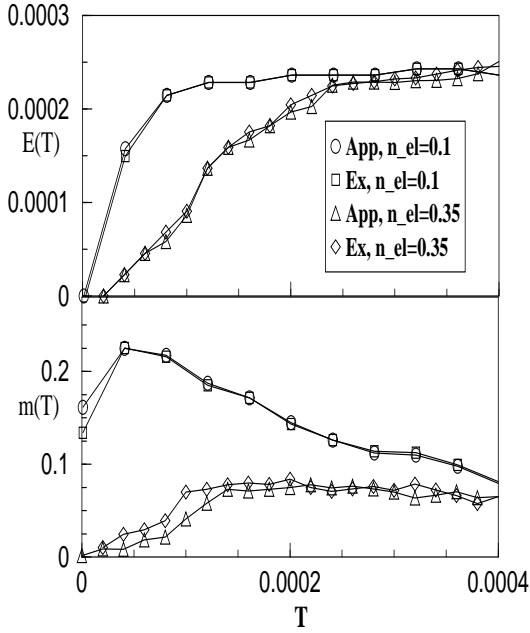


FIG. 2. Exact simulation -vs- Monte Carlo with H_{sp} : clean system. $J' = 0.2$, $h = 10^{-5}$. The data is averaged over 1000 configurations at each T , after equilibration over 1000 steps. Total energy (top panel) and magnetisation (lower panel). System size 4^3 . There is a spin at each site: $N_{sp} = N$.

The symbols are the ‘exact’ cost, the quadratic curves (firm lines) are the approximate cost. It is obvious that even in the worst case the ‘exact’ and ‘approximate’ results match very well upto $J' \sim 0.2$.

Since this configuration based testing cannot be exhaustive, we have run the full simulation, using the exact scheme, and also done MC with H_{sp} , to check if the thermodynamics and magnetism come out similar in the two approaches. We have used $J' = 0.2$ and studied a 4^3 clean system (Fig.2) as well as a system with strong disorder (Fig.3). We think the similarity is quite convincing. We have also studied $J' = 1$ (not shown) where the difference is quite significant.

The principal conclusion from these tests is that we can reliably use an effective quadratic Hamiltonian for the spins, and there are no polaronic effects in the parameter regime we are in.

B. Results on transport

To calculate the conductivity and compare with experimental data we would have to do a MC on the spin problem, having computed the J_{ij} , and use the Kubo formula. The conductivity will have to be averaged over equilibrium spin configurations. To compute the MR, *i.e.* $\sigma(h)$, the magnetic problem has to be redone in the presence of the field, and the cycle repeated. Even after

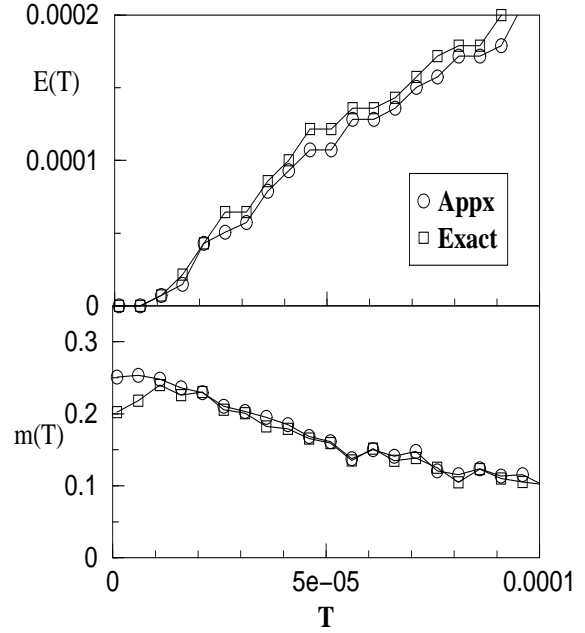


FIG. 3. Exact simulation -vs- Monte Carlo with H_{sp} : disordered system. $\Delta = 8$, $J' = 0.2$, $n_{el} = 0.1$, $h = 10^{-6}$, size 4^3 , $N_{sp} = N$. The data is averaged over 1000 configurations at each T , after equilibration over 1000 steps. Energy (upper panel) and magnetisation (lower panel).

the approximation we have made, this is a time consuming process. In this paper we do not discuss those results, saving it for the discussion specific to GdSi, but highlight some simple limiting cases.

We want to illustrate the interplay of structural and spin disorder, and the difference in σ between a spin polarised and random system.

The conductivity is plotted in arbitrary units, *i.e.* without putting in e^2/h and the lattice parameter.

1. Effect of on site disorder

First consider the case with only ‘on site’ disorder. This is the traditional Anderson localisation problem. We use the Kubo-Greenwood formula³⁵ to calculate σ . The data in Fig.4 displays the variation in conductivity (as ϵ_F is varied) and the DOS, with increasing disorder. $\sigma(\epsilon)$ is the variation in conductivity as the electron density, or ϵ_F , is varied. It is not the ‘optical’ conductivity.

The inset in Fig.4 shows the variation in the maximum conductivity in the band (σ_{max} say) which occurs at the band center here, with increasing disorder. Note the precipitous drop (even in this finite size calculation). The most recent numerical calculations³⁶ put the Anderson transition in the 3d tight binding model at $\Delta \sim 16.5$.

To study localisation near the band edge we need to follow the size dependence of the conductivity for a fixed ϵ (or electron density). If states at a certain energy, ϵ , are localised then $\sigma(\epsilon : L)$ will decrease with increasing L (exponentially at large L). If the states are extended

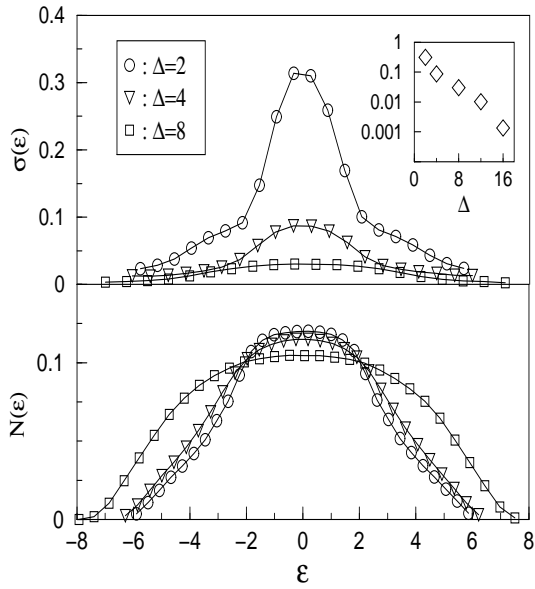


FIG. 4. Effect of on site disorder: conductivity (upper panel) and DOS (lower panel) in the presence of site disorder. System size $6 \times 6 \times 16$. The inset shows σ_{max} the conductivity at the band center as a function of increasing disorder; notice that the σ scale is logarithmic. The data is averaged over 200 – 600 realisations of disorder depending on Δ .

then $\sigma(\epsilon : L)$ will tend to a finite asymptote as $L \rightarrow \infty$. Fig.5 shows $\sigma(\epsilon : L)$ for system size $6 \times 6 \times L$, with $L = 16$ and 32 , for two strengths of disorder. The crossing point is a crude measure of the mobility edge separating extended and localised states. $\sigma(\epsilon : L)$ is approximately

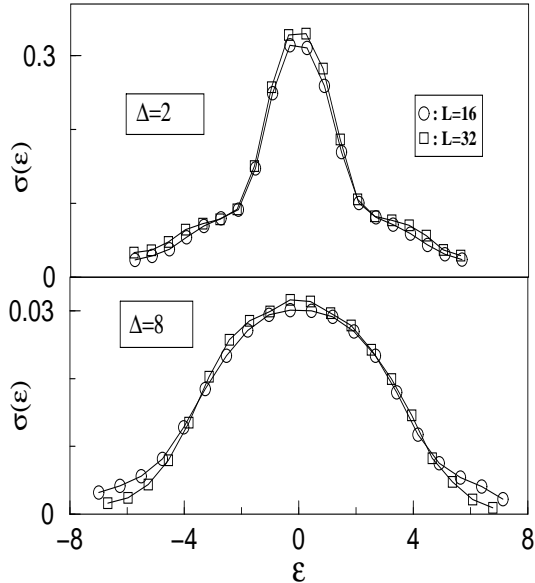


FIG. 5. System size dependence of the ‘conductivity’, at two values of disorder, $\Delta = 2$ and 8 . The system sizes are $6 \times 6 \times 16$ and $6 \times 6 \times 32$. Average over 200 – 600 realisations of disorder depending on system size and Δ . Notice the crossing of the curves in each panel.

independent of L for states in the center of the band, implying that our system size is large enough to provide an estimate of the conductivity in the thermodynamic limit.

The purpose of presenting these results on the very standard site disorder problem is (i) to validate our conductivity calculation, and (ii) to make an estimate of the fraction of states localised as a function of disorder Δ . As a crude estimate, 15% of the states (in the band tails) get localised for $\Delta \sim 8$. This will be useful for fixing parameter values in the GdSi problem.

2. Effect of ‘spin disorder’: uncorrelated spins

Now consider how electron scattering off random magnetic moments affect the conductivity. We consider a periodic array of spins with random orientations. This mimics an (uncorrelated) paramagnetic state. There is no on site disorder. The conductivity, computed by diagonalising the electron problem in these random background, is shown in Fig.6 for three values of J' . The data is averaged over 100 spin configurations for each J' . Remember that to compute the conductivity of an electron system coupled to spins, the spin distribution has to be *computed*, a non trivial task. Here we just *assumed* an uncorrelated random distribution. This is expected to provide an estimate of σ in the spin glass phase (with $h = 0$). The inset in the top panel shows the reduction in the maximum conductivity with increasing J' .

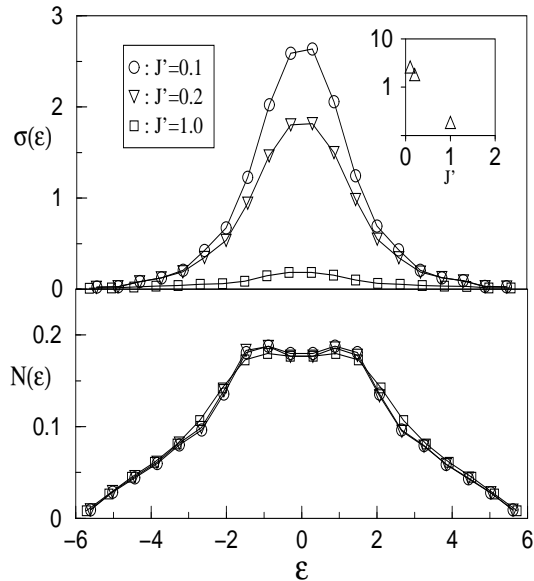


FIG. 6. Effect of ‘spin disorder’: conductivity (upper panel) and DOS (lower panel) for electrons coupled to randomly oriented spins. The exchange coupling is $J' = 0.1, 0.2$ and 1.0 and there is a spin at each site. There is no on site disorder. Inset in the upper panel shows reduction in band center conductivity with increasing J' . System size $6 \times 6 \times 16$. Data averaged over 100 spin configurations.

A similar problem, with $J'/t \rightarrow \infty$, has been studied earlier³⁷ in the context of the double exchange model. System size dependence of the conductivity in our results does not indicate localisation in the band tails (upto errors $\sim 1\%$). In the $J' \rightarrow \infty$ problem³⁷ it is known that less than 1% of the states are localised in the tail of the band. Principally, in the small J' limit in which we have calculated the conductivity, electron coupling to ‘spin disorder’ leads to a finite scattering rate $\sim N(\epsilon_F)J'^2$, and a small resistivity, and not much by way of localisation.

We suspect that the mean free path at $J' = 0.1$ and 0.2 is probably too large, $l_{mfp} \gtrsim L$, to reproduce the ‘infinite volume’ conductivity.

3. On site and ‘spin disorder’: spin at each site

The problem relevant for us has both on site and spin disorder. Fig.7 shows the interplay of these two effects. The top curve in the upper panel corresponds to on site disorder only, $\Delta = 8$. The lower curve (squares) shows the additional effect of random spins, coupled to the electrons with $J' = 0.2$. If we focus on the band center, for instance, the *resistivity* increases from $\sim 1/0.03$ to $\sim 1/0.015$, *i.e.* from ~ 33 to ~ 66 (in arb units). This *difference*, call it $\Delta\rho_{sp}$, arises due to spin disorder. What would be the resistivity if *only* this spin disorder were operative? This can be seen from the lower panel in Fig.7. The ‘spin disorder only’ resistivity, ρ_{sp}^0 is $\sim 0.5 \ll \Delta\rho_{sp}$, which is two orders of magnitude larger.

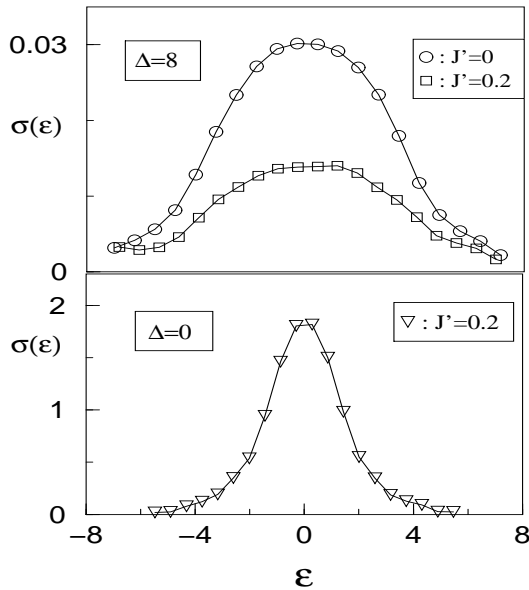


FIG. 7. Interplay of on site disorder and spin disorder: conductivity in the presence of a random on site potential and randomly oriented spins *on a lattice* ($N_{sp} = N$). Top panel shows data with on site disorder only ($\Delta = 8$ circles), and on site + spin disorder ($\Delta = 8, J' = 0.2$, squares). The bottom panel shows σ for $J' = 0.2$, as in Fig. 6, without any on site disorder.

We think that ρ_{sp}^0 is being underestimated, since $l_{mfp} \gtrsim L$. Nevertheless, even with a factor of 2 error, the difference between ρ_{sp}^0 and $\Delta\rho_{sp}$ is still significant.

In this disorder regime, the ‘on site’ and ‘spin disorder’ effects are far from additive: there is no Mathiessen’s rule. This would of course be obvious close to the mobility edge, where spin disorder will lead to localisation of additional states, but it is also prominently visible at the band center.

Within the accuracy of our calculation we have not been able to see the shift in the mobility edge on introducing spin disorder (the shift, again, would be $\lesssim 1\%$). However, as noted, even in the regime of *extended states*, there is a dramatic increase in resistivity on introducing randomly oriented spins, quite out of proportion to the small coupling, $J' = 0.2$.

The change in σ (circles to squares, Fig.7) is, crudely, the difference between YSi and GdSi: *i.e.* the effect of on site disorder -vs- on site + spin disorder. This also provides an impression of the magnetoconductance obtainable, at large field. The $J' = 0$ curve on the top panel is also the conductivity for *fully polarised moments* (in which case the coupling becomes irrelevant).

4. On site and ‘spin disorder’: dilute random array of spins

Now for the final degree of realism. Consider the effect of randomly *locating* the spins (as in any amorphous structure) together with random orientation, Fig.8. There is also strong structural disorder in the background, $\Delta = 8$. There are three sources of randomness in this problem, in the site disorder $\{\epsilon_i\}$, the spin locations

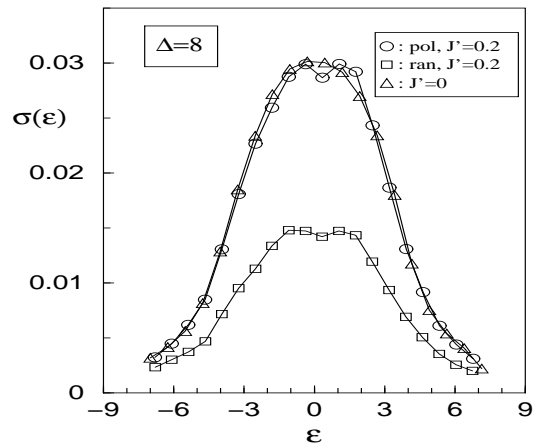


FIG. 8. Interplay of on site disorder and spin disorder: conductivity in the presence of a random on site potential and *randomly located* array of spins. The fraction of sites with spins is $n_{sp} = 0.3$, the disorder is $\Delta = 8$ and the system size is $6 \times 6 \times 16$. The bottom curve (squares) corresponds to random orientation of the spins, one of the top curves (circles) corresponds to fully polarised spins, both with $J' = 0.2$. The third set (triangles) corresponds to on site disorder only ($\Delta = 8, J' = 0$) and is displayed for comparison.

$\{\mathbf{R}_i\}$, and the orientations $\{\mathbf{S}_i\}$. The $\{\mathbf{R}_i\}$'s were on a lattice in Fig.7. The data reveals that the effect of randomly locating the moments is of no consequence when the moments are polarised, σ looks as if there are no moments at all (top two curves). This is because of the strong structural disorder already present. Polarised moments only ‘renormalise’ the structural disorder from Δ to approximately $\sqrt{\Delta^2 + J'^2} \approx \Delta$. Disorder in the *orientation* however has a strong effect, just as for periodically located spins, and all our arguments about MR, in the last section, are applicable here as well. The difference between the top curve(s) and the lower curve would be the ‘magnetoconductance’ at strong field. We are doing a more extensive calculation to quantify the localisation effects near the mobility edge.

C. Magnetic moments in the electron system: effect of increasing disorder

The previous section set out some of the limits for the conductivity, arising from site disorder and randomly oriented or fully polarised spins. For these results to have any relevance the actual magnetic state in the system should bear some resemblance to the random magnetic state we used. In this section we study the magnetic state that arises for moments coupled to electrons in a disordered environment, and the conditions under which a ‘spin glass’ state can arise. We first consider a periodic system, *i.e* one with a spin on each site of the lattice and study the thermodynamic and magnetic properties as the disorder, Δ , is increased.

1. Periodic array of spins

The magnetic properties are studied via Monte Carlo on the Hamiltonian $H_{sp} = \sum_{i \neq j} J_{ij} \mathbf{S}_i \cdot \mathbf{S}_j$ as discussed earlier. The J_{ij} depend on electron density, J' , and the *specific realisation of disorder in ϵ_i 's*. For a clean system, $\Delta = 0$, the bonds J_{ij} depend only on the separation $i - j$ irrespective of the location of the two sites. More concretely, when using periodic boundary conditions (PBC), all nearest neighbour bonds will have the same value J_1 , next nearest neighbour bonds will all be J_2 , and so on.

The bond *distribution* for nearest neighbour bonds, call it $P_1(J)$ will be a δ function. Similarly $P_2(J)$, for next nearest neighbours, $P_3(J)$, for third neighbours, will all be δ functions. These bond distributions broaden out when the electron system is disordered.

The bond distribution, upto third neighbour, is shown on Fig.9 for a 6^3 system, with PBC, for $\Delta = 2, 4$, and 8 . The ‘spikes’ are the ‘distribution’ for $\Delta = 0$. Notice that although the first neighbour coupling remains ferromagnetic from $\Delta = 0$ to 8 , the farther neighbour couplings are antiferromagnetic and not much weaker than the first neighbour coupling (at strong disorder).

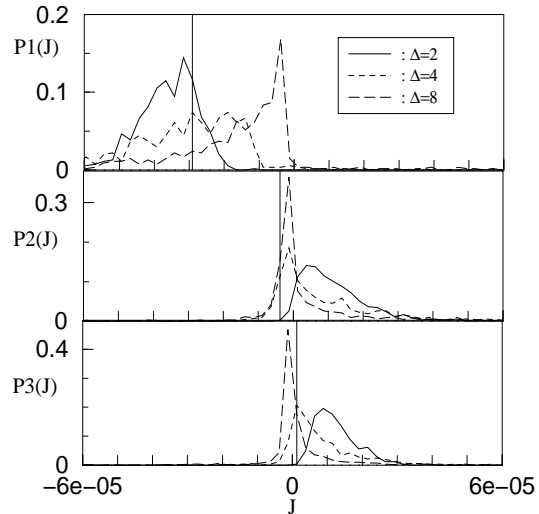


FIG. 9. Distribution of bonds: nearest neighbour, $P_1(J)$, next neighbour, $P_2(J)$, and third neighbour, $P_3(J)$, as a function of increasing disorder. The spins are on a 6^3 lattice, the electron density is 0.1 and $J' = 0.2$. The spikes (δ functions) correspond to the clean case ($\Delta = 0$). The bonds are calculated for a single realisation of disorder for each Δ . The normalising factor for all the distributions is 4×10^5 .

The clean system is a model case of ‘RKKY’, with some difference arising from the finite size and ‘lattice’ nature of the system. The strongly disordered systems also seem to have reasonably long range interactions³⁸, but frustrating instead of regular as in the RKKY case.

The next figure, Fig.10, shows the result of simulations on H_{sp} . The internal energy $E(T)$ and the weak field magnetisation $m(T)$ are monitored. The data is averaged

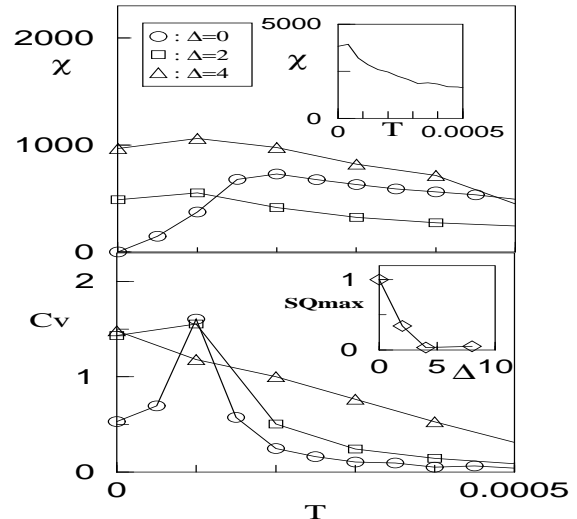


FIG. 10. Susceptibility, specific heat, and structure factor in the bond disordered periodic magnetic system. Upper panel, susceptibility (χ), lower panel, specific heat (C_V), for increasing disorder, $\Delta = 0, 2, 4$. The system size 6^3 , $J' = 0.2$, and $n_{el} = 0.1$. The upper inset shows χ for $\Delta = 8$, and the lower panel shows the evolution of the *peak amplitude* in the structure factor, $S(\mathbf{q})$, with increasing disorder.

over ~ 1000 equilibrium configurations at each temperature and then over 2 – 8 realisations of disorder, depending on Δ . The following are the important features in the data: (i) All the way from $\Delta = 0$ to $\Delta = 8$ there is a cusp in the susceptibility. The temperature at which it occurs reduces from $\sim 1.8 \times 10^{-4}$ at $\Delta = 0$, to 0.5×10^{-4} at $\Delta = 8$ (see inset in top panel, Fig.10). (ii) The magnetic specific heat has a well defined peak at $\Delta = 0$, which gets broadened with increasing disorder. The specific heat is larger in the bond disordered systems at lower temperature. It is useful to remember that these are *classical* spins, so the C_V remains finite at $T = 0$, (iii) the feature in χ and C_V suggests an ordering transition in the clean system, while the nature of the low temperature state in the disordered systems is not obvious purely from C_V and χ . Since the spins are on a periodic structure, we calculated the structure factor $S(\mathbf{q})$ from the ground state configuration in each case (inset, lower panel). (iii) The clean system has a single peak in $S(\mathbf{q})$ at $\mathbf{q} = 0, 0, \pi$, of magnitude $\sim \mathcal{O}(N^2)$. The system is ordered as expected. A reduced peak survives at the same \mathbf{q} for $\Delta = 2$, see Fig.10, but disappears at larger disorder. The feature in χ , along with the absence of any long range order, suggests that the strongly disordered systems are actually spin glasses. We are in the process of computing the Edwards-Anderson order parameter and checking the system size dependence of our results on χ and $S(\mathbf{q})$.

2. Dilute random array of spins

Finally, let us look at the magnetism in a site diluted clean system. This would be the canonical RKKY model

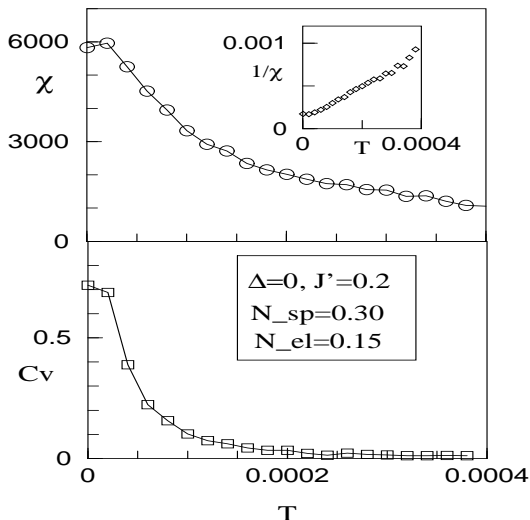


FIG. 11. Susceptibility and specific heat in the *clean* diluted spin system. The spins are distributed on randomly chosen 30% of the sites in a 8^3 system. The electron density is 0.15, $J' = 0.2$ and $\Delta = 0$. Applied field $h = 10^{-5}$. The data is averaged over 1000 MC steps at each temperature after equilibration over 1000 steps.

except that the real exchange in a lattice model looks somewhat different from the simple $r^{-3}\cos(2k_F r)$ form usually assumed in simulating such models. We show the χ and C_V in such a system, an 8^3 lattice with spins on 30% of the sites. χ has the same cusp, as in Fig.10, flattening at low temperature, probably indicative of spin glass freezing. We are studying the spin glass order parameter for this problem, as well as the effect of on site disorder. There has been some work on RKKY spin glasses in three dimension^{39–41} but the results about a spin glass transition (in the absence of anisotropy) are still inconclusive. There is no work, to the extent we know, on models with site dilution as well as disorder.

V. CONCLUSIONS

We wanted to explore the interplay of structural disorder and doped magnetic moments in an electron system within a simple model. Though we are far from demonstrating the experimentally observed features near the i-m-t, or detailed properties of the observed spin glass, we have highlighted how strong disorder can generate most of these effects. For instance, relatively weak ‘spin disorder’ (*i.e.* small J'), acting *on top of* structural disorder, can have remarkable effects on transport. This spin disorder acting on its own, in a high density electron system, would have led only to weak scattering, masked by electron-phonon effects etc. Here the change $\Delta\rho$ is large, and so is the MR. Similarly, the occurrence of a *disordered* magnetic state, which is the key to the i-m-t and MR, is again facilitated by structural disorder. We saw how this happens, due to frustration, for a periodic array of spins. We have not shown results on the actual temperature and field dependence of transport, we will discuss these separately¹⁹. Most importantly, we have not provided a hint of how Coulomb effects can be incorporated. Let us provide a qualitative discussion.

A controlled perturbative scheme⁸ for handling e-e effects exists at weak disorder. This should allow an understanding of the metallic phase, far from the transition, *in terms of the spectrum and wavefunctions computed in our scheme*. Similarly, deep in the insulator, a knowledge of the localisation length and screening allows us to quantify the effects of e-e interactions²⁰. There is no detailed theory which allows us to access physical properties near the i-m-t (see the work¹⁰ by V. Dobrosavljevic and G. Kotliar though), although there are RG calculations (reviewed⁹ by Belitz and Kirkpatrick). There is also an interesting scheme⁴² suggested by Kuchinskii *et al.* but the ‘control’ in their procedure is not obvious. So, although it seems difficult to start completely from first principles, including e-e and electron-spin interactions, an understanding of our simplified model can help in quantifying the e-e effects in the problem.

VI. ACKNOWLEDGMENT

One of us (P.M) would like to thank T. V. Ramakrishnan for a discussion, and the Isaac Newton Institute, Cambridge, for hospitality during part of this work.

-
- ¹ N. F. Mott and E. A. Davis, *Electronic Processes in Non Crystalline Materials*, Clarendon Press, Oxford (1979).
- ² N. F. Mott, *Metal-Insulator Transitions*, Taylor & Francis, London (1990).
- ³ P. W. Anderson, Phys. Rev. **109**, 1498 (1958).
- ⁴ P. A. Lee and T. V. Ramakrishnan, Rev. Mod. Phys. **57**, 287 (1985).
- ⁵ M. P. Sarachik in *Metal-Insulator Transitions Revisited*, Ed. P. P. Edwards and C. N. R. Rao, Taylor & Francis, London (1995).
- ⁶ R. F. Milligan, T. F. Rosenbaum, R. N. Bhatt and G. A. Thomas in *Electron-Electron Interactions in Disordered Systems*, ed. A. L. Efros and M. Pollak, North Holland (1985).
- ⁷ G. Hertel, D. J. Bishop, E. G. Spencer, J. M. Rowell and R. C. Dynes, Phys. Rev. Lett. **50**, 743 (1983).
- ⁸ See the review by B. L. Altshuler and A. G. Aronov in *Electron-Electron Interactions in Disordered Systems*, ed. A. L. Efros and M. Pollak, North Holland (1985).
- ⁹ See the review by D. Belitz and T. R. Kirkpatrick, Rev. Mod. Phys. **66**, 261 (1994), for a summary of current understanding.
- ¹⁰ See V. Dobrosavljevic and G. Kotliar, Phys. Rev. Lett. **78**, 3943 (1997), for a recent approach to the problem.
- ¹¹ T. Kasuya and A. Yanase, Rev. Mod. Phys. **40**, 684 (1968).
- ¹² P. A. Wolff, in *Semiconductors and Semimetals, Vol. 25*, Ed. Willardson and Beer, Academic Press (1988).
- ¹³ S. von Molnar, A. Briggs, J. Floquet and G. Remenyi, Phys. Rev. Lett. **51**, 706 (1983).
- ¹⁴ H. Ohno, H. Munekata, T. Penney, S. von Molnar and L. L. Chang, Phys. Rev. Lett. **68**, 2664 (1992).
- ¹⁵ F. Hellman, M. Q. Tran, A. E. Gebala, E. M. Wilcox and R. C. Dynes, Phys. Rev. Lett. **77**, 4652 (1996).
- ¹⁶ B. L. Zink, E. Janod, K. Allen and F. Hellman, Phys. Rev. Lett. **83**, 2266 (1999).
- ¹⁷ F. Hellman, D. R. Queen, R. M. Potok and B. L. Zink Phys. Rev. Lett. **84**, 5411 (2000).
- ¹⁸ W. Teizer, F. Hellman and R. C. Dynes, Phys. Rev. Lett. **85**, 848 (2000).
- ¹⁹ Sanjeev Kumar and Pinaki Majumdar, to be published.
- ²⁰ A. L. Efros and B. I. Shklovskii, J. Phys. **C8**, L49 (1975), and in *Electron-Electron Interactions in Disordered Systems*, ed. A. L. Efros and M. Pollak, North Holland (1985).
- ²¹ W. Teizer, F. Hellman and R. C. Dynes, Sol. St. Comm. **114**, 81 (2000).
- ²² P. Xiong, B. L. Zink, S. I. Appelbaum, F. Hellman and R. C. Dynes, Phys. Rev. B **59**, R3929 (1999).
- ²³ M. A. Paalanen, J. E. Graebner, R. N. Bhatt and S. Sachdev, Phys. Rev. Lett. **61**, 597 (1988).
- ²⁴ M. Milovanovic, S. Sachdev and R. N. Bhatt, Phys. Rev. Lett. **63**, 82 (1989).
- ²⁵ K. Binder and A. P. Young, Rev. Mod. Phys. **58**, 801 (1986).
- ²⁶ K. H. Fischer and J. A. Hertz, *Spin Glasses*, Cambridge (1991).
- ²⁷ J. A. Mydosh, *Spin Glasses*, Taylor & Francis (1993).
- ²⁸ E. Dagotto, S. Yunoki, A. L. Malvezzi, A. Moreo, J. Hu, S. Capponi, D. Poiblanc and N. Furukawa, Phys. Rev. **B 58**, 6414 (1998).
- ²⁹ M. J. Calderon and L. Brey, cond-mat 9801311.
- ³⁰ H. Yi, N. H. Hur and J. Yu, cond-mat 9910153.
- ³¹ Y. Motome and N. Furukawa, cond-mat 0007407, July 2000.
- ³² J. L. Alonso, L. A. Fernandez, F. Guinea, V. Laliena and V. Martin-Mayor, cond-mat 0007450, July 2000.
- ³³ C. Kittel, *Quantum Theory of Solids*, John Wiley and Sons (1963).
- ³⁴ See, e.g. Patrik Fazekas, *Lecture Notes on Electron Correlation and Magnetism*, World Scientific (1999), pp 641.
- ³⁵ The Kubo formula for d.c conductivity in the non interacting case is discussed in Mott and Davis¹. There are some problems in an actual numerical implementation of this scheme because the eigenstates are typically ‘real’ and non degenerate in the cases we consider. In the infinite volume limit the states will be quasi-degenerate and the conductivity (at fixed ϵ_F) can be computed from this manifold. In our finite system we compute $\sigma(\epsilon)$ by considering two successive states in the spectrum.
- ³⁶ K. Slevin, T. Ohtsuki and T. Kawarabayashi, Phys. Rev. Lett. **84**, 3915 (2000).
- ³⁷ Q. Li, J. Zang, A. R. Bishop and C. M. Soukoulis, Phys. Rev. **B 56**, 4541 (1997).
- ³⁸ A. Jagannathan, E. Abrahams and M. J. Stephen, Phys. Rev. B. **37**, 5522 (1988).
- ³⁹ A. J. Bray, M. A. Moore and A. P. Young, Phys. Rev. Lett. **56**, 2641 (1986).
- ⁴⁰ A. Chakrabarti and C. Dasgupta, Phys. Rev. Lett. **56**, 1404 (1986).
- ⁴¹ F. Matsubara and M. Iguchi, Phys. Rev. Lett. **68**, 3781 (1992).
- ⁴² E. Z. Kuchinskii, M. V. Sadovskii, V. G. Suvorov and M. A. Erkabaev, JETP. **80**, 1122 (1995).